

# UC Riverside

## UC Riverside Previously Published Works

### Title

Selective Supramolecular Porphyrin/Fullerene Interactions1

### Permalink

<https://escholarship.org/uc/item/5tp8m4fx>

### Journal

Journal of the American Chemical Society, 121(45)

### ISSN

0002-7863

### Authors

Boyd, Peter DW  
Hodgson, Michael C  
Rickard, Clifton EF  
[et al.](#)

### Publication Date

1999-11-01

### DOI

10.1021/ja992165h

Peer reviewed

# Selective Supramolecular Porphyrin/Fullerene Interactions<sup>1</sup>

Peter D. W. Boyd,\*<sup>‡</sup> Michael C. Hodgson,<sup>†</sup> Clifton E. F. Rickard,<sup>†</sup> Allen G. Oliver,<sup>†</sup> Leila Chaker,<sup>†</sup> Penelope J. Brothers,<sup>†</sup> Robert D. Bolskar,<sup>‡</sup> Fook S. Tham,<sup>‡</sup> and Christopher A. Reed\*<sup>‡</sup>

Contribution from the Department of Chemistry, The University of Auckland, Private Bag 92019, Auckland, New Zealand, and Department of Chemistry, University of California Riverside, Riverside, California 92521-0403

Received June 24, 1999

**Abstract:** Naturally assembling cocrystallates of C<sub>60</sub> and C<sub>70</sub> fullerenes with tetraphenylporphyrins (H<sub>2</sub>TPP·C<sub>60</sub>·3 toluene, **1**; H<sub>2</sub>T<sub>3,5</sub>-dibutylPP·C<sub>60</sub>, **2**; H<sub>2</sub>T<sub>3,5</sub>-dimethylPP·1.5C<sub>60</sub>·2 toluene, **3**; H<sub>2</sub>T<sub>piv</sub>PP·C<sub>60</sub>, **4**; H<sub>2</sub>T<sub>3,5</sub>-dimethylPP·C<sub>70</sub>·4 toluene, **5**; ZnTPP·C<sub>70</sub>, **6**; NiT<sub>4</sub>-methylPP·2C<sub>70</sub>·2 toluene, **7**) show unusually short porphyrin/fullerene contacts (2.7–3.0 Å) compared with typical π–π interactions (3.0–3.5 Å). In the C<sub>60</sub> structures, an electron-rich, 6:6 ring juncture, C–C bond lies over the center of the porphyrin ring. In the C<sub>70</sub> structures, the ellipsoidal fullerene makes porphyrin contact at its equator rather than its poles; a carbon atom from three fused six-membered rings lies closest to the center of the porphyrin. These structures provide an explanation for the manner in which tetraphenylporphyrin-appended silica stationary phases effect the chromatographic separation of fullerenes. The interaction of the curved π surface of a fullerene with the planar π surface of a porphyrin, without the need for matching convex with concave surfaces, represents a new recognition element in supramolecular chemistry. NMR measurements show that this interaction persists in toluene solution, suggesting a simple way to assemble van der Waals complexes of donor–acceptor chromophores.

## Introduction

The curved π surface of C<sub>60</sub> shows a tendency to interact with other molecules, making it an interesting target for engineering supramolecular arrays. In the early structural chemistry of fullerenes, cocrystallizations with ferrocene, S<sub>8</sub>, and SbPh<sub>3</sub>, etc. were important for obtaining ordered crystal structures.<sup>2</sup> Fullerenes are particularly soluble in methylated arenes,<sup>3</sup> and the visible spectrum of C<sub>60</sub> shows considerable solvatochromism.<sup>4</sup> Host–guest chemistry of fullerenes using calixarenes etc. has been developed to effect separations,<sup>5</sup> modify redox behavior,<sup>6</sup> and entrap C<sub>60</sub> in a container.<sup>7</sup> Matching a concave host to the convex fullerene surface is believed to enhance binding.

Related to this activity has been the development of tetraphenylporphyrin-appended silica stationary phases for the chromatographic separation of fullerenes.

With columns of these materials, Meyerhoff has reported selectivity superior to the commonly used “Buckyclutcher”<sup>8</sup> and “Buckyprep”<sup>9</sup> columns.<sup>10</sup> The basis of the separation is proposed to be a π–π interaction between zinc tetraphenylporphyrin and the fullerene.<sup>11</sup>

In a recent crystal structure of a covalently linked tetraphenylporphyrin–C<sub>60</sub> dyad we made the first observation of a close fullerene/porphyrin contact suggesting an attraction of C<sub>60</sub> to the center of a porphyrin ring.<sup>12</sup> This seemed to support the suggestion of a special interaction but the association could have been an accident of crystal packing because the fullerene and porphyrin were rigidly tethered.

We now show that this association is ubiquitous in untethered cocrystallates of fullerenes and tetraphenylporphyrins and that this type of interaction occurs in solution.

## Results and Discussion

**X-ray Structures with C<sub>60</sub>.** Slow evaporation of toluene solutions containing a 1:1 ratio of C<sub>60</sub> and a variety of tetraarylporphyrins give binary materials containing both chromophores. Cocrystallization was readily determined by the observation of new crystal habits, different from those of the individual components. Alternatively, randomly selected crystals could be dissolved in toluene to reveal visible spectra that were the summation of the fullerene and porphyrin components. From several data sets on a number of crystalline compounds, the X-ray structures of four cocrystallates have been determined.

\* Corresponding authors: (phone) (CAR) 909-787-5197; (fax) (CAR) 909-787-2435; (e-mail) (CAR) chris.reed@ucr.edu (PDWB) pdw.boyd@auckland.ac.nz.

<sup>†</sup> The University of Auckland.

<sup>‡</sup> University of California.

(1) Abbreviations used in this paper: H<sub>2</sub>TPP = tetraphenylporphyrin; H<sub>2</sub>T<sub>3,5</sub>-dibutylPP = tetrakis(3,5-di-*tert*-butylphenyl)porphyrin; H<sub>2</sub>T<sub>3,5</sub>-dimethylPP = tetra(3,5-dimethylphenyl)porphyrin; H<sub>2</sub>T<sub>piv</sub>PP = tetra(*o*-pivalamido)porphyrin (“picket fence” porphyrin); H<sub>2</sub>T<sub>4</sub>-methylPP = tetra-*p*-tolylporphyrin.

(2) Ferduco, M.; Olmstead, M. M.; Fawcett, W. R. *Inorg. Chem.* **1995**, *34*, 390–392, and references therein.

(3) Ruoff, R. S.; Tse, D. S.; Malhotra, R.; Lorents, D. C. *J. Phys. Chem.* **1993**, *97*, 3379–3383.

(4) Gallagher, S. H.; Armstrong, R. S.; Lay, P. A.; Reed, C. A. *J. Phys. Chem.* **1995**, *99*, 5817–5825.

(5) (a) Suzuki, T.; Nakashima, K.; Shinkai, S. *Chem. Lett.* **1994**, 699–703. (b) Atwood, J. L.; Koutsantonis, G. A.; Raston, C. L. *Nature (London)* **1994**, *368*, 229–231.

(6) Olsen, S. A.; Bond, A. M.; Compton, R. G.; Lazarev, G.; Mahon, P. J.; Marken, F.; Raston, C. L.; Tedesco, V.; Webster, R. D. *J. Phys. Chem. A* **1998**, *102*, 2641–2649.

(7) (a) Yanase, M.; Haino, T.; Fukazawa, Y. *Tetrahedron Lett.* **1999**, *40*, 2781–2784. (b) Ikeda, A.; Yoshimura, M.; Udzu, H.; Fukuhara, C.; Shinkai, S. *J. Am. Chem. Soc.* **1999**, *121*, 4298–4299.

(8) Welch, C. J.; Pirkle, W. H. *J. Chromatogr.* **1992**, *609*, 89–101.

(9) Kimata, K.; Hosoya, K.; Araki, T.; Tanaka, N. *J. Org. Chem.* **1993**, *58*, 282–283.

(10) Xiao, J.; Meyerhoff, M. E. *J. Chromatogr. A* **1995**, *715*, 19–29.

(11) Xiao, J.; Savina, M. R.; Martin, G. B.; Francis, A. H.; Meyerhoff, M. E. *J. Am. Chem. Soc.* **1994**, *116*, 9341–9342.

(12) Sun, Y.; Drovetskaya, T.; Bolskar, R. D.; Bau, R.; Boyd, P. D. W.; Reed, C. A. *J. Org. Chem.* **1997**, *62*, 3642–3649.

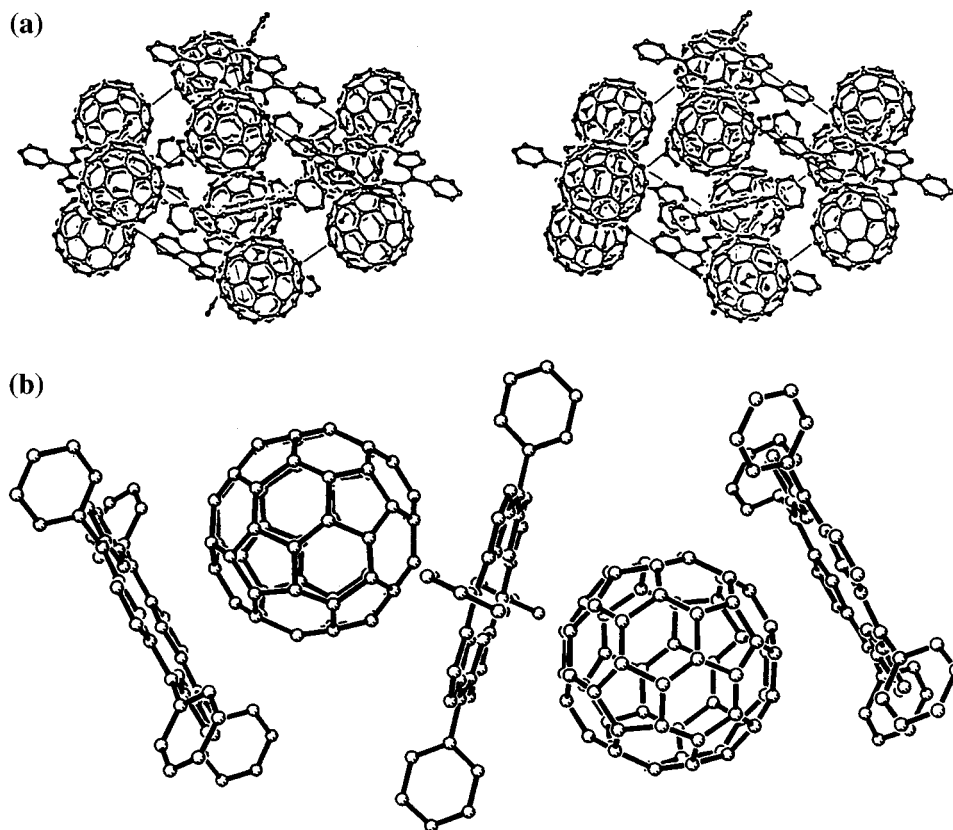


**Figure 1.** (a) Stereoview of packing diagram for H<sub>2</sub>TPP·C<sub>60</sub>·3 toluene, **1**. One of the disordered C<sub>60</sub> and the two ordered toluene molecules are displayed. (b) View of fragment of porphyrin/C<sub>60</sub> chain in **1**.

The structure of H<sub>2</sub>TPP·C<sub>60</sub>·3 toluene, **1**, reveals a zigzag chain of alternating porphyrin/C<sub>60</sub> interactions (see Figure 1). As shown in Figure 2, C<sub>60</sub> is centered over the porphyrin with electron-rich 6:6 ring-juncture C–C bonds in close approach to the plane of the porphyrin core (C to mean 24-atom plane distances = 2.70, 2.77, 2.75, and 2.98 Å). The closest atom-to-atom contacts are from the two 6:6 fullerene carbon atoms to the porphyrin N atoms. They range from 3.09 to 4.74 Å. The phenyl carbon atoms of the porphyrin are all at distances >4.0 Å from fullerene carbon atoms, indicating that the ortho C–H bonds do not contribute significantly to the association. The angle between the porphyrin planes is 45.2°. The remaining exposed surface of C<sub>60</sub> is solvated by the methyl groups of lattice toluene, the methyl carbon to fullerene carbon distances lying in the range 3.39–3.59 Å. The closest carbon-to-carbon atom distance between fullerenes in adjacent chains is 3.37 Å.

With 3,5-di-*tert*-butyl groups on the tetraphenylporphyrin, a very similar zigzag assembly crystallizes (see Figure 3). H<sub>2</sub>T<sub>3,5-dibutyl</sub>PP·C<sub>60</sub>, **2**, is unsolvated with the *tert*-butyl groups fulfilling the same role as the toluene in **1**. The closest methyl carbon to fullerene carbon atom distances are in the range 3.6–4.0 Å. The orientation of C<sub>60</sub> is very similar to that found in **1** with the 6:6 ring junction carbon atoms lying over the center of the porphyrin ring at distances of 2.69–2.88 Å from the porphyrin plane. The angle between the porphyrin planes is 45.3°. Interestingly, there are no close fullerene/fullerene contacts.

With 3,5-di-methyl groups on the tetraphenylporphyrin, a 1:1.5 cocrystallate forms in H<sub>2</sub>T<sub>3,5-dimethyl</sub>PP·1.5C<sub>60</sub>·2 toluene, **3**. As found in **1** and **2**, there is a 1:1 porphyrin/C<sub>60</sub> zigzag chain, a close interaction of the porphyrin core with the 6:6 ring junction of C<sub>60</sub>, and methyl group/fullerene solvation (see Figure 4). A further, crystallographically independent C<sub>60</sub> molecule (0.5

equiv.) is solvated entirely by methyl groups from eight surrounding porphyrin molecules.

A facially encumbered tetraphenylporphyrin such as “picket fence” porphyrin (H<sub>2</sub>T<sub>piv</sub>PP) cocrystallizes with C<sub>60</sub> from toluene as the unsolvated H<sub>2</sub>T<sub>piv</sub>PP·C<sub>60</sub>, **4**. The X-ray structure reveals a close C<sub>60</sub>–porphyrin approach to the unencumbered side of the porphyrin plane (see Figure 5). A linear chain is formed with C<sub>60</sub> nestled into the *tert*-butyl groups from pivalamide pickets of an adjacent porphyrin. Adjacent linear chains alternate in a direction such that phenyl groups from the porphyrins solvate fullerenes in adjacent chains. The repeating porphyrin cores are coplanar in this structure, suggesting that the zigzag arrangements in **1**–**3** are dictated by packing efficiency.

**X-ray Structures with C<sub>70</sub>.** With C<sub>70</sub>, H<sub>2</sub>T<sub>3,5-dimethyl</sub>PP gives crystals of composition H<sub>2</sub>T<sub>3,5-dimethyl</sub>PP·C<sub>70</sub>·4 toluene, **5**. As shown in Figure 6, it too has a chain of alternating porphyrin/fullerene interactions. The porphyrin planes are parallel, leading to a linear chain structure. Notably, the C<sub>70</sub> balls are sandwiched in a “side-on” manner with respect to the porphyrin planes. As shown in Figure 7, the unique C<sub>70</sub> carbon atom at the junction of three fused six-membered rings in the equatorial belt lies closest to the center of the porphyrin ring (C to mean 24-atom plane distance = 2.86 Å). Two adjacent carbon atoms are the next closest at 2.95 and 3.01 Å. This apparently maximizes van der Waals contact. It contrasts with “end-on” coordination to metals where  $\pi$ -back-bonding interactions are important.<sup>13</sup> Lattice toluene molecules occupy channels between the linear chains, completely solvating the fullerene with methyl groups from eight toluene molecules (see Figure 6).

C<sub>70</sub> cocrystallizes with the zinc(II) complex of H<sub>2</sub>TPP giving ZnTPP·C<sub>70</sub>, **6**, whose X-ray crystal structure now shows a zigzag

(13) Balch, A. L.; Olmstead, M. M. *Chem. Rev.* **1998**, *98*, 2123–2166.

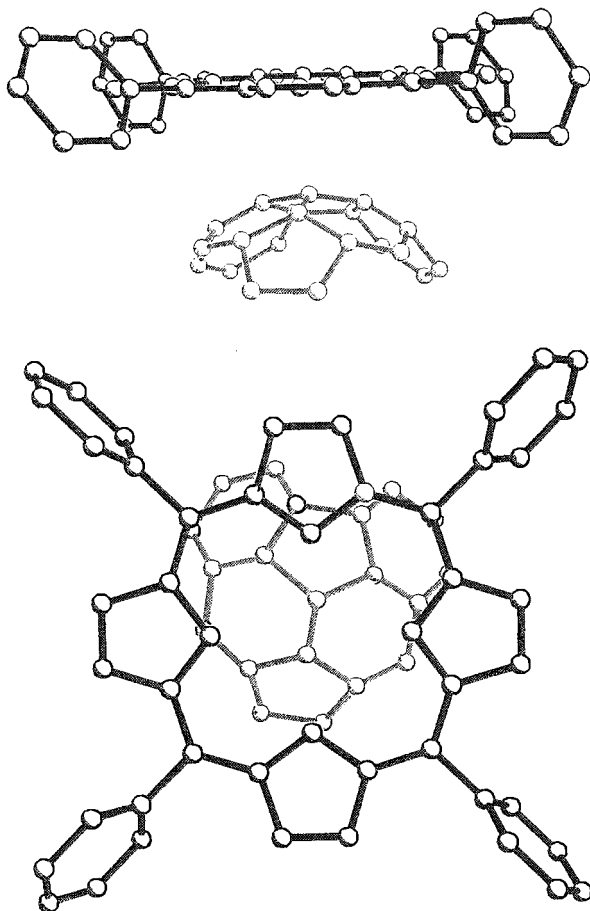


**Figure 2.** Orientation of  $C_{60}$  with respect to porphyrin plane in **1**. For clarity, the fullerene is in gray scale.

chain of porphyrin and  $C_{70}$  molecules (see Figure 8). The  $C_{70}$  molecule adopts the same “side-on” orientation as seen in the nonmetalated analogue, **5**. The closest  $C_{70}$  carbon atom to the porphyrin plane is again that at the junction of three fused six-membered rings. The Zn–C distance is 2.89 Å, slightly shorter than the sum of the van der Waals radii (3.09 Å). This raises the question of whether there is a contribution to the interaction from fullerene-zinc coordinate bonding. A weak fullerene-iron coordinate bond has recently been postulated in  $[Fe(TPP)(C_{60})][F_{20}-BPh_4] \cdot 2.5$  dichlorobenzene as evidenced by a small out-of-plane displacement of the iron atom from the mean plane of the porphyrin core.<sup>14</sup> This is observable because the complex is five-coordinate. In **6**, however, the fullerene interaction occurs equally on both sides of the porphyrin so it is not possible to separate six coordination from van der Waals interactions. The approach of  $C_{70}$  to the porphyrin in metalated **6** is very similar to that in unmetalated **5**, despite the large gross differences in lattice organization. This leads us to conclude that although fullerene-zinc coordinate bonding may be present, it is weak compared with the van der Waals interaction.

$C_{70}$  also cocrystallizes with the nickel(II) complex of tetrap-tolylporphyrin giving  $NiT_{4-methyl}PP \cdot 2C_{70} \cdot 2$  toluene, **7**. The X-ray structure reveals two crystallographically independent fullerene molecules in the asymmetric unit (see Figure 9). One  $C_{70}$  is asymmetrically situated between two crystallographically distinct porphyrins and adopts the same “side-on” orientation seen in compounds **5** and **6** to one of these porphyrins. This  $C_{70}$  is disordered and has been successfully modeled using two

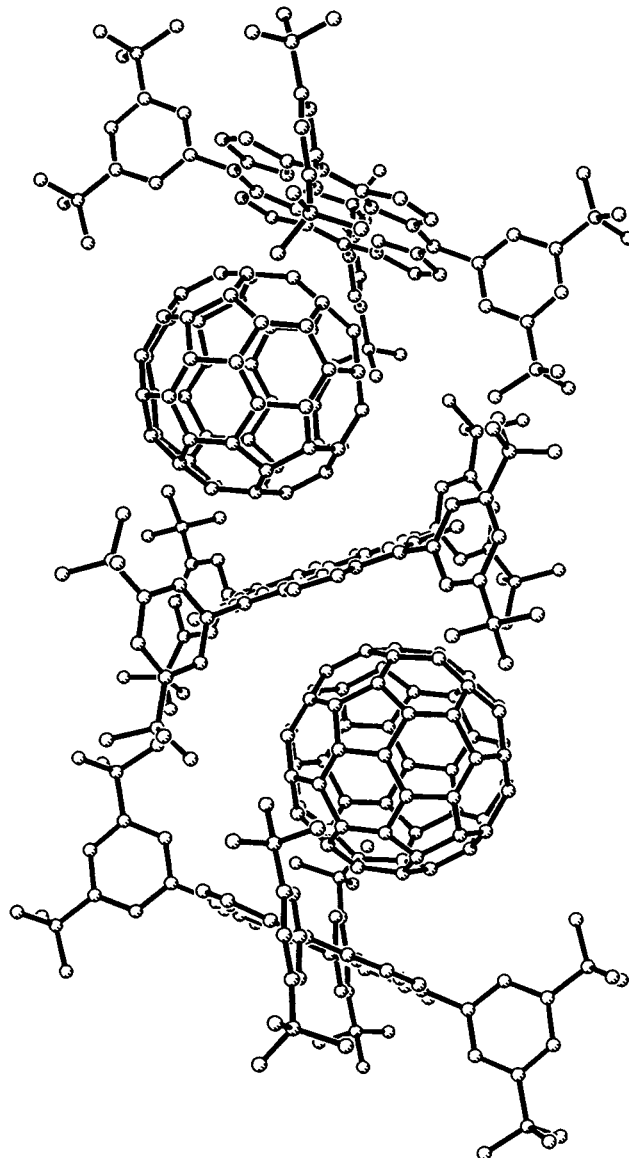


**Figure 3.** Fragment of porphyrin/ $C_{60}$  chain in the crystal structure of  $H_2T_{3,5-dibutyl}PP \cdot C_{60}$ , **2**, with one of the disordered  $C_{60}$  chains displayed.

$C_{70}$  fullerene orientations (canted  $41^\circ$  relative to one another, see Experimental Section), of 76% and 24% occupancy, respectively. The metal atom is close to a  $C_{70}$  carbon atom at the junction of three fused six-membered rings for one of the nickel porphyrins, this distance being 2.96 Å for the 76% occupied  $C_{70}$  and 2.85 Å for the 24% occupied  $C_{70}$ . Similar to **6**, but unlike **5**, the porphyrin planes asymmetrically sandwiching this  $C_{70}$  molecule are not parallel ( $33.5^\circ$ ). The opposite porphyrin nickel atom has its close approach not to a  $C_{70}$  carbon atom at the junction of three fused six-membered rings, but to one at the fusion of one five-membered ring and two six-membered rings (closer to the “pole” of the  $C_{70}$ ) at distances of 3.04 and 2.99 Å for the 76% and 24% occupied fullerenes, respectively. The separate, distinct  $C_{70}$  molecule, which is more ordered, occupies the cavity between adjacent porphyrins, with its closest approach to a phenyl plane of a  $NiT_{4-methyl}PP$  tolyl group being 3.3 Å. The asymmetric unit contains two toluene molecules, one of which is disordered with disorder occupancy factors of 85% and 15%. With respect to all of the fullerene-porphyrin cocrystallates discussed, the structure of  $NiT_{4-methyl}PP \cdot 2C_{70} \cdot 2$  toluene uniquely manifests the subtle

(14) Evans, D. R.; Fackler, N. L. P.; Xie, Z.; Rickard, C. E. F.; Boyd, P. D. W.; Reed, C. A. *J. Am. Chem. Soc.* **1999**, *121*, 8466–8474.

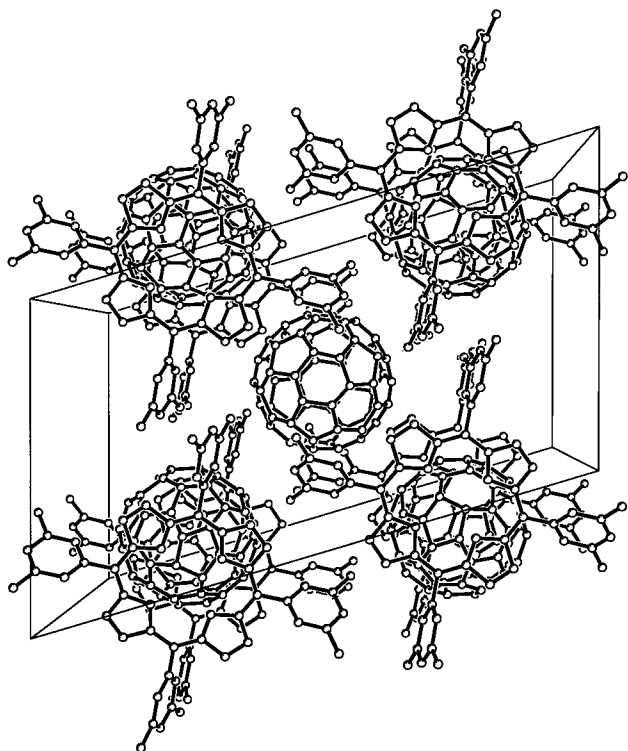


**Figure 4.** Partial packing diagram for  $\text{H}_2\text{T}_{3,5\text{-dimethyl}}\text{PP}\cdot 1.5\text{C}_{60}\cdot 2$  toluene, **3**, showing the two crystallographically distinct fullerenes. The porphyrin-complexed  $\text{C}_{60}$  molecules make a square; the methyl-group-solvated  $\text{C}_{60}$  is in the center.

interplay between the favorable fullerene–porphyrin van der Waals interactions and overall packing considerations.

**The Fullerene–Porphyrin Interaction.** Metrical data for all seven structures are gathered in Table 1. The most important feature of these structures is their unexpectedly close porphyrin/fullerene contact. Typical fullerene/arene or porphyrin/arene  $\pi$ – $\pi$  interactions lie in the range 3.0–3.5 Å,<sup>15</sup> whereas each of the present structures have at least one fullerene carbon atom within 2.75–2.96 Å of the porphyrin plane (see C–P<sub>24</sub> distances in Table 1). The close approach indicates a particularly favorable attractive interaction between the porphyrin and fullerene chromophores and explains the ease with which these assemblies form. In all four  $\text{C}_{60}$  structures, the closest approaching fullerene carbon atoms are those from an electron-rich 6:6 ring-juncture C–C bond. In the three  $\text{C}_{70}$  structures, the closest approaching fullerene carbon atoms are those at the most electron-rich site—the intersection of three fused, six-membered rings. This suggests that van der Waals dispersion forces are the critical component of the interaction. The greater fullerene/porphyrin contact provided by the side-on rather than end-on orientation of  $\text{C}_{70}$  is also consistent with the importance of dispersion forces. Attraction of the fullerene to the center of the porphyrin, as opposed to elsewhere on the  $\pi$  surface, is probably the result of packing efficiency but it may also reflect a small component of electrostatic energy. The center of a porphyrin or metalloporphyrin is electron-deficient compared with the olefinic bonds of fullerenes, making  $\text{C}_{60}$  the donor. This contradicts the general molecular notion of fullerenes being strong electron acceptors but is understandable at the microscopic level.

Using force field methods,<sup>16,17</sup> molecular modeling of  $(\text{H}_2\text{TTP})_x(\text{C}_{60})_y$  and  $(\text{H}_2\text{TTP})_x(\text{C}_{70})_y$  clusters gives rise to the

(15) Typical distances are given in refs 21–25 of ref 14.

(16) Calculations carried out using CERIU 2, version 3.5, 1997; Molecular Simulations: San Diego, CA.

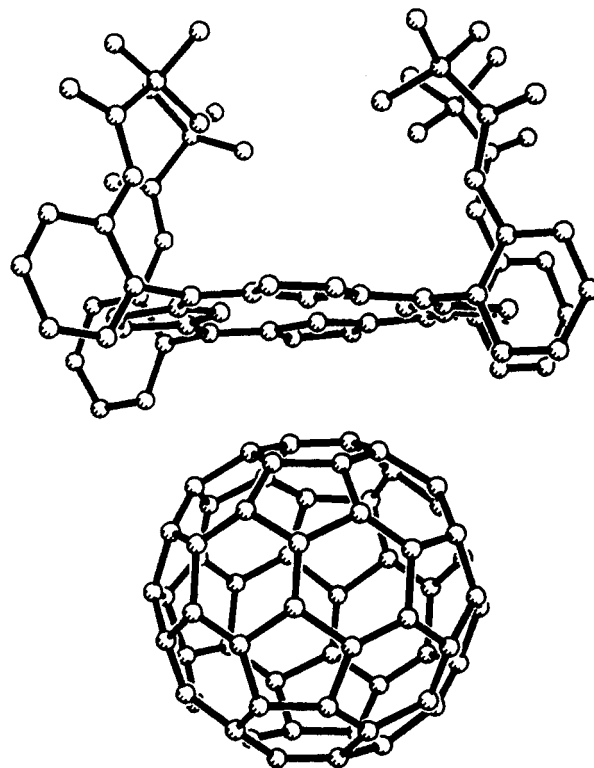


**Figure 5.** Linear stacking of  $\text{H}_2\text{T}_{\text{piv}}\text{PP}$  with  $\text{C}_{60}$  in the crystal structure of  $\text{H}_2\text{T}_{\text{piv}}\text{PP}\cdot\text{C}_{60}$ , **4**, with one of the disordered  $\text{C}_{60}$  molecules displayed.

same kinds of chains seen in the X-ray structures. Figure 10 shows the computed structure for  $x = 3$  and  $y = 4$  in a porphyrin/ $\text{C}_{60}$  cluster. The structures of these clusters show the close approach of the porphyrin to the 6:6 C–C bonds of  $\text{C}_{60}$  and the equatorial six-membered rings of  $\text{C}_{70}$ . The nearest fullerene to porphyrin mean plane distances are 2.85–2.90 Å for  $\text{C}_{60}$  and 2.76 Å for  $\text{C}_{70}$ . The calculated closest atom–atom contacts in the porphyrin/ $\text{C}_{60}$  clusters are the porphyrin N $\cdots$ C distances of  $\sim 3.1$  Å, while in the porphyrin/ $\text{C}_{70}$  clusters contacts of 3.14 Å are observed. These are all in good agreement with distances observed in the X-ray structures (see Table 1). The computed angles between the porphyrins in the zigzag chains are larger than observed,  $\sim 75^\circ$  for  $\text{C}_{60}$  and  $\sim 40^\circ$  for  $\text{C}_{70}$ .

(17) Universal Force Field, version 1.02: Rappé, A. K.; Casewit, C. J.; Colwell, K. S.; Goddard, W. A.; Skiff, W. M. *J. Am. Chem. Soc.* **1992**, *114*, 10024–10035. PCFF Force Field: Hwang, M. J.; Stockfisch, T. P.; Hagler, A. T. *J. Am. Chem. Soc.* **1994**, *116*, 2515–2525; Sun, H.; Mumby, S. J.; Maple, J. R.; Hagler, A. T. *J. Am. Chem. Soc.* **1994**, *116*, 2978–2987; Sun, H.; Mumby, S. J.; Maple, J. R.; Hagler, A. T. *J. Phys. Chem.* **1995**, *99*, 5873–5882.

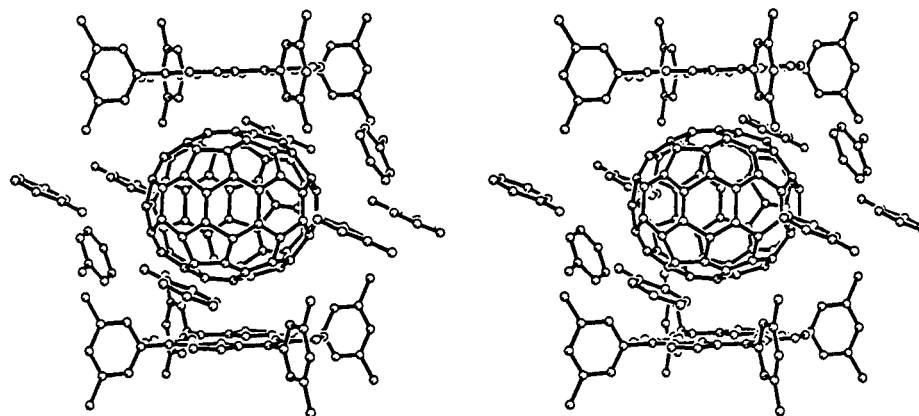


**Figure 6.** Stereoview of a molecular packing diagram for  $\text{H}_2\text{T}_{3,5\text{-dimethyl}}\text{PP}\cdot\text{C}_{70}\cdot 4$  toluene, **5**, with one of the disordered  $\text{C}_{70}$  molecules displayed.

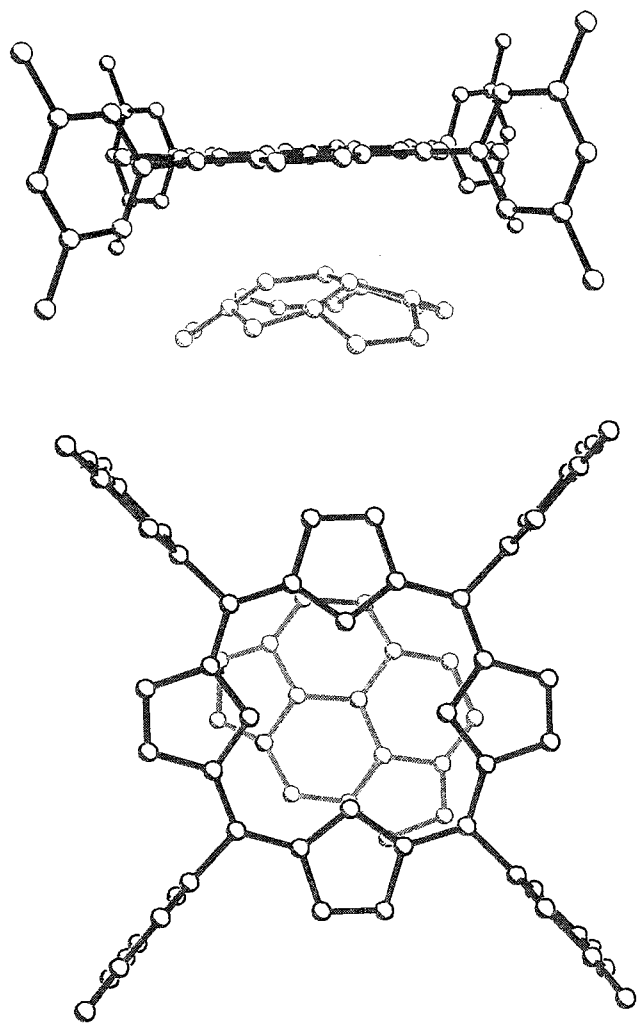


**Figure 7.** Orientation of  $\text{C}_{70}$  with respect to the porphyrin plane in **5**. For clarity, the fullerene is in gray scale.

The energy of interaction between  $\text{C}_{60}$  and tetraphenylporphyrin was calculated to be 33.6 and 28.0 kcal/mol for the Universal and PCFF force fields, respectively, while for  $\text{C}_{70}$  the interaction was calculated to be 31.9 and 28.9 kcal/mol, respectively. In both cases, the major contribution to the fullerene/porphyrin binding energy was found to originate in the van der Waals terms of the force field. In the case of the Universal force field, the van der Waals contribution was about 95%. For the PCFF force field, it was about 80%. The remaining contributions correspond to electrostatic interactions between the porphyrin molecules.

Semiempirical and minimal basis ab initio molecular orbital calculations<sup>18</sup> on  $\text{C}_{60}$ /porphine ( $\text{C}_{20}\text{H}_{14}\text{N}_4$ ) do not reproduce the close approach, giving instead separations of the order of 3.3–3.4 Å. This is an expected result if the interaction is primarily van der Waals in nature since neither of these calculations takes into account electron correlation. However, density-functional calculations with nonlocal corrections for correlation<sup>19</sup> do reproduce the close interaction of the two chromophores. A preliminary geometry optimization (rms gradient 0.0013 Hartree/Å) of a  $\text{C}_{60}$ /porphine cluster showed a close approach of the 6:6 bond of  $\text{C}_{60}$  to the porphyrin with a separation of  $\sim 2.8$  Å and C–N contacts of 3.14–3.26 Å, comparable to the experimentally determined distances. The calculated binding energy, relative to the energies of the optimized fullerene and porphyrin, is 5.8 kcal/mol. For comparison, the calculated binding energies of fullerene/porphine clusters using structural parameters from the X-ray structures of **1** are 7.7 kcal/mol. Although these binding energies are significantly less than those estimated from the force-field methods, it is well-known that density functional methods do not reproduce binding energies very well when dealing with dispersive forces.

**Porphyrin- $\text{C}_{60}$  Interactions in Solution.** Even though fullerenes and tetraphenylporphyrins cocrystallize with great ease, one could still argue that the way they approach each other in the solid state is dictated more by size, shape, and packing considerations than by the special affinity we highlight above. For this reason, we investigated the attraction of  $\text{C}_{60}$  to a porphyrin in solution. Toluene was chosen as solvent primarily to obtain practical levels of solubility for NMR studies but it serves another important purpose: As an excellent solvent for both  $\text{C}_{60}$  and porphyrin, any fullerene/porphyrin attraction must compete with potentially superior fullerene/toluene and porphyrin/toluene solvent interactions. The choice of a more polar solvent would undoubtedly promote the aggregation of the hydrophobic fullerene and porphyrin entities but this could be viewed as an artificial enhancement of their affinity. The demonstration of fullerene/porphyrin binding in toluene solution is therefore considered a particularly stringent test of spontaneous attraction.

Toluene solutions of  $\text{C}_{60}$  and tetraphenyl- or tetra(3,5-di-*tert*-butylphenyl)-porphyrin show UV–visible spectra that are simply the sum of the spectra of the two individual chromophores. This suggests that electronic spectroscopy is insensitive to complex

(18) Full geometry optimizations using the semiempirical PM3 model and the ab initio Hartree-Fock method with a minimal STO-3G basis set using Spartan 4.0; Wave function Inc.: Irvine, CA 92612.

(19) ADF 2.3.0, Theoretical Chemistry, Vrije Universiteit, Amsterdam. (a) Baerends, E. J.; Ellis, D. E.; Ros, P. *Chem. Phys.* **1973**, *2*, 41–51. (b) te Velde, G.; Baerends, E. J. *J. Comput. Phys.* **1992**, *99*, 84–98.

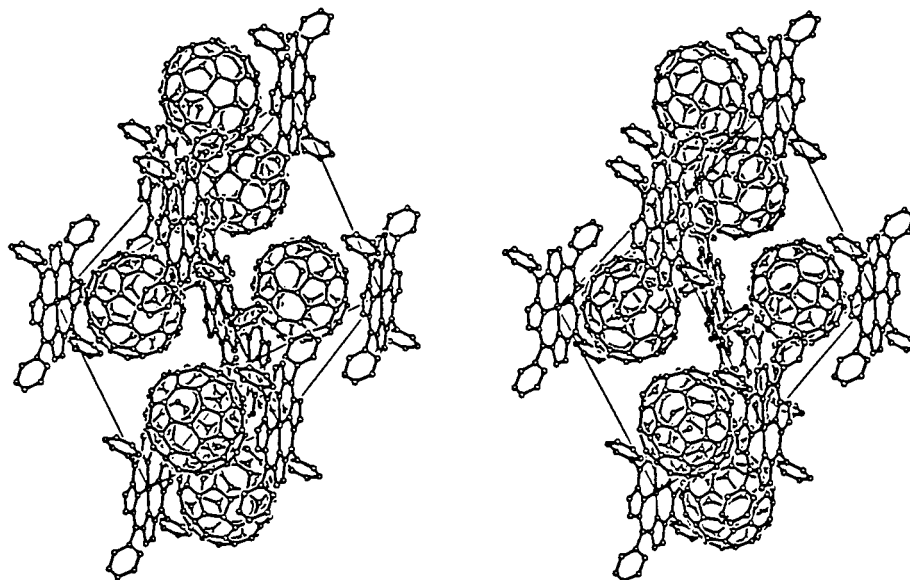


**Figure 8.** Stereoview of a molecular packing diagram for ZnTPP·C<sub>70</sub>, **6**, with one of the disordered C<sub>70</sub> molecules displayed.

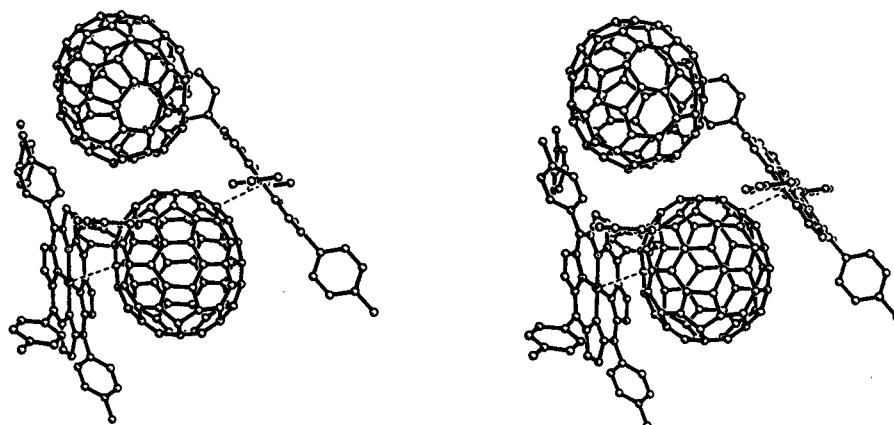


**Figure 9.** Stereoview of a molecular packing diagram for NiT<sub>4</sub>-methylPP·2C<sub>70</sub>·2 toluene, **7**, showing both types of C<sub>70</sub> molecules. The depicted C<sub>70</sub> molecule between the porphyrin planes is the 76% occupied disorder model.

**Table 1.** Selected Structural Parameters

structure	porphyrin plane–Fullerene distances (<3.2 Å) <sup>a</sup>	Porphyrin–Porphyrin angle (deg) <sup>b</sup>	Fullerene–Fullerene contact <sup>c</sup>	Porphyrin–Fullerene contacts (Å) <sup>d</sup>
<b>1</b>	2.75, 2.99, 3.05, 3.07 <sup>e</sup> , 2.72, 2.79, 3.11, 3.14	45.2	3.37	3.02, 3.11, 3.10, 3.12
<b>2</b>	2.69, 2.83, 2.97, 3.11, 3.19, 2.69, 2.88, 3.02, 3.04	45.3	5.49	3.03, 3.06, 3.14
<b>3</b>	2.92, 2.87, 3.01, 3.14, 2.71, 2.72, 2.95, 3.12	31.6	3.59	2.88 (2×), 3.07 (2×), 3.1 (2×)
<b>4</b>	2.82 (2×), 3.08 (2×) <sup>f</sup> , 2.74 (2×), 3.11 (2×) <sup>g</sup>		6.30	3.08 (2×)
<b>5</b>	2.86, 2.95, 3.01	0.0	5.67	3.04, 3.13, 3.19, 3.20
<b>6</b>	2.80, 2.93, 3.16, 3.21, 2.82, 2.81, 3.02, 3.12	41.1	5.71	3.13, 3.15, 3.18, 3.19 2.89 (2×), <sup>h</sup> 2.86, 3.03
<b>7</b>	2.96, <sup>i</sup> 2.97, <sup>i</sup> 3.04, <sup>i</sup> 2.85, <sup>j</sup> 2.99, <sup>j</sup> 3.19 <sup>j</sup>	33.5	3.42	3.11, <sup>k</sup> 3.12, <sup>l</sup> 3.15 <sup>l</sup>

<sup>a</sup> Distance from the mean plane of the 24-atom porphyrin core. <sup>b</sup> Angle between the mean planes of the porphyrins (24-atom cores). <sup>c</sup> Closest carbon–carbon distance. <sup>d</sup> Porphyrin N to fullerene C distances <3.2 Å. <sup>e</sup> Distances for one of disordered C<sub>70</sub> molecules. <sup>f</sup> Distance to first disordered C<sub>60</sub>. <sup>g</sup> Distance to second disordered C<sub>60</sub>. <sup>h</sup> Zinc to fullerene C distances <3.2 Å. <sup>i</sup> Nickel to fullerene C distance for the 76% occupied C<sub>70</sub>, <3.2 Å. <sup>j</sup> Nickel to fullerene C distance for the 24% occupied C<sub>70</sub>, <3.2 Å. <sup>k</sup> Porphyrin N to fullerene C distance for the 76% occupied C<sub>70</sub>, <3.2 Å. <sup>l</sup> Porphyrin N to fullerene C distances for the 24% occupied C<sub>70</sub>, <3.2 Å.

formation and/or that the degree of association is weak. However, NMR studies of such solutions show mutually upfield shifts in both the <sup>13</sup>C spectrum of C<sub>60</sub> and the <sup>1</sup>H spectrum of the porphyrin N–H protons, indicative of complex formation. For example, a 1:1 solution of C<sub>60</sub>/H<sub>2</sub>TPP at 3.3 × 10<sup>-2</sup> M concentration gives shifts of 0.09 and 0.04 ppm, respectively, while for C<sub>60</sub>/H<sub>2</sub>T<sub>3,5</sub>-dibutylPP shifts of 0.21 and 0.05 ppm are observed. These shifts are small but real. No other peaks are affected so the shifts cannot be ascribed to a bulk solvent effect or to collision-induced shielding. Titration of a toluene/CS<sub>2</sub> (4:1

v/v) solution of C<sub>60</sub> (2 mM) with H<sub>2</sub>T<sub>3,5</sub>-dibutylPP leads to a monotonic change in the <sup>13</sup>C position with added porphyrin ranging from 0.17 to 0.86 ppm for 1:1 through 1:5 C<sub>60</sub>/porphyrin mole ratios. The average chemical shift for C<sub>60</sub> in close approach to a porphyrin, as found in the X-ray structures of **1**, **2**, **3**, and **4**, can be estimated using the measured diamagnetic anisotropy of H<sub>2</sub>TPP<sup>20</sup> and the carbon-atom positions. This leads to an average upfield shift of 2.81 ppm. All of the carbon atoms in

(20) Murray, K. S.; Sheahan, R. M. *Aust. J. Chem.* **1975**, *28*, 2623–2628.

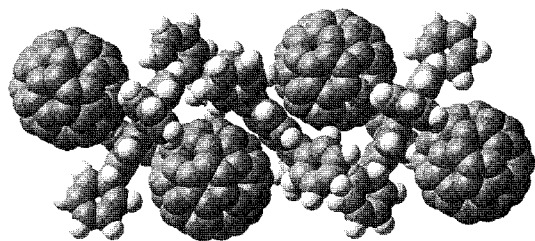


**Figure 10.** Molecular mechanics model of a porphyrin- $C_{60}$  cluster  $(H_2TTP)_3(C_{60})_4$  calculated using the PCFF force field.

the fullerene are shifted upfield because they all subtend less than the “magic angle” with respect to the normal to the porphyrin plane.

Attempts were made to analyze these shifts in terms of Job plots for complex formation but no clear stoichiometry could be distinguished. Estimates of the amount of complex formed based on the assumption of a 1:1 complex range from 5 to 30% depending on the porphyrin and relative concentrations.

## Conclusions

This work reveals that the close contacts between fullerenes and porphyrins arise from a favorable van der Waals attraction of the curved  $\pi$  surface of a fullerene to the planar  $\pi$  surface of a porphyrin. The phenomenon appears to be quite general and can be observed in solution as well as the solid state. While this work was in progress, related observations were reported in the solid state for complexes of octaethylporphyrin.<sup>13,21</sup> A fullerene/ $\pi$  interaction has also been observed with dimethylamino-substituted porphyrazines.<sup>22</sup> Our calculations suggest that dispersion forces are the fundamental basis of these interactions.

These results offer a basis for chromatographic selectivity of tetraphenylporphyrin-appended silica phases in effecting separations of fullerenes.<sup>11</sup> The longer retention time of  $C_{70}$  relative to  $C_{60}$  correlates with the greater van der Waals contact of  $C_{70}$  seen in the present structures.  $C_{70}$  can be viewed as two hemispheres of  $C_{60}$  with the insertion of an equatorial belt of graphitelike hexagons, creating a flattening at the equator. This flattening allows a greater porphyrin/fullerene contact area as long as the interaction is side-on rather than end-on. Estimation of the solvent-accessible surface areas of 1:1  $C_{60}$  and  $C_{70}$  tetraphenylporphyrin clusters from structures **1** and **5** give contact areas of 90.2 and 98.6 Å<sup>2</sup>, respectively.

Inspection of the present structures reveals favorable solvation of  $C_{60}$  and  $C_{70}$  by aliphatic groups. This is apparently the next most important interaction in these systems, after  $\pi$ - $\pi$  interactions, and is consistent with the relative solubility of  $C_{60}$  and  $C_{70}$  in arenes versus alkanes.<sup>23</sup>

The curved  $\pi$  surface of the fullerene has given rise to a new type of supramolecular recognition element *without the necessity of matching a concave host with a complementary convex guest*. This can potentially be exploited in crystal engineering and supramolecular assembly. It is significant that the fullerene/porphyrin association can be demonstrated in toluene solution. By increasing the interaction strength with solvents more polar than toluene and by manipulating the porphyrin substituents, it

should be possible to construct molecular assemblies for photophysical applications. In contrast to covalently linked dyads, porphyrin–fullerene conjugates of this type can have a truly noncovalent<sup>24</sup> association of chromophores. This more closely mimics the tetrapyrrolic “special pair” and antenna pigments of the biological photosystem reaction center.

## Experimental Section

**Porphyrin/Fullerene Cocrystallizations.** Toluene solutions containing equimolar amounts of fullerene and porphyrin or metalloporphyrin were allowed to evaporate slowly at room temperature. Cocrystallates appeared to form quantitatively from these solutions as they evaporated, giving crystals suitable for X-ray studies. The visible spectrum of randomly selected crystals dissolved in toluene showed the superposition of the spectra of the individual chromophores.

**X-Ray Structure Determinations.** Intensity data for **1–6** were recorded on a Siemens SMART diffractometer with a CCD area detector at The University of Auckland. Data for **1–6** were corrected for Lorentz and polarization effects and absorption corrections applied using multiple symmetry equivalent reflections.<sup>25</sup> The X-ray structural study on **7** was conducted at the University of California, Riverside and is described below.

Structures **1–6** were solved by direct methods using SHELXS-97<sup>26</sup> and refined on  $F^2$  using SHELXL-97.<sup>27</sup> In all cases, the porphyrin moieties were clearly defined in the initial E-maps. While the positions of the fullerenes were clear, the resolution was poorer, and it was apparent that they were disordered.

In the cases of **1**, **2** and **4** it was possible to resolve two disordered  $C_{60}$  moieties. In structure **1**, the electron density maps were fitted to the known structure of  $C_{60}$ <sup>28</sup> and the resultant structures refined as rigid groups.<sup>29</sup> Two solvent toluene molecules were also resolved; however, after the final refinement four peaks of  $\sim 2 \text{ e } \text{Å}^{-3}$  remained. These appeared to correspond to a disordered toluene molecule, but no satisfactory model could be constructed to account for this. To further investigate this, the SQUEEZE function of the program PLATON<sup>30</sup> was used to examine the cavity containing the disordered solvent. It was found that the integrated total electron density and the corresponding volume of the cavity corresponded well to one toluene molecule. A final refinement was carried out using reflections modified by the SQUEEZE procedure. Structure **2** was refined in a manner similar to **1** using a rigid group refinement of the disordered fullerenes. For structure **4**, the fullerenes were disordered about the 2-fold monoclinic axis, and these were refined with the restriction that equivalent bonds in the fullerenes were equal (SHELX SADI).

Structure **3** was more complex, containing two crystallographically independent fullerenes. Each fullerene was found to be disordered with respect to symmetry elements of the space group  $C2/m$  but it was possible to construct a model for this disorder. As in structure **1**, it was found that further electron density due to two disordered toluene solvent molecules was present. A final refinement for this structure, using data modified by the PLATON program, was carried out with constraints on the 6:6 and 5:6 bond lengths of the two fullerenes (SHELX DFIX).

The porphyrin molecules in structures **5** and **6** were well-defined. In structure **5**, the  $C_{70}$  molecule showed a 2-fold disorder with respect

(24) The term “non-covalent” is frequently used in supramolecular chemistry to describe species that associate via coordinate bonds to metal complexes. Since even the weakest of coordinate bonds have some covalence we view this terminology as misleading.<sup>14</sup>

(25) Blessing, R. H. *Acta Crystallogr.* **1995**, *A51*, 33–38.

(26) Sheldrick, G. M. Program for the solution of crystal structures; University of Göttingen: Germany, 1997.

(27) Sheldrick, G. M. Program for the refinement of crystal structures; University of Göttingen: Germany, 1997.

(28)  $C_{60}$ : Bürgi, H. B.; Blanc, E.; Schwarzenbach, D.; Liu, S.; Lu, Y.; Kappes, M. M.; Ibers, J. A. *Angew. Chem., Int. Ed. Engl.* **1992**, *31*, 640–643;  $C_{70}$ : Bürgi, H. B.; Venugopalan, P.; Schwarzenbach, F.; Dieterich, F.; Thilgen, C. *Helv. Chim. Acta* **1993**, *76*, 2155–2159.

(29) Spek, A. L. *Acta Crystallogr.* **1990**, *A46*, C34.

(30) Sluis, P. V. D.; Spek, A. L. *Acta Crystallogr.* **1990**, *A46*, 194.

(21) Olmstead, M. M.; Costa, D. A.; Maitra, K.; Noll, B. C.; Phillips, S. L.; Van Calcar, P. M.; Balch, A. L. *J. Am. Chem. Soc.* **1999**, *121*, 7090–7097.

(22) Eichhorn, D. M.; Yang, S. L.; Jarrell, W.; Baumann, T. F.; Beall, L. S.; White, A. J. P.; Williams, D. J.; Barrett, A. G. M.; Hoffman, B. M. *J. Chem. Soc., Chem. Commun.* **1995**, 1703–1704.

(23) Beck, M. T.; Mándi, G. *Fullerene Sci. Tech.* **1997**, *5*, 291–310.



to an inversion center. The fullerene was refined with constraints on the C<sub>70</sub> molecule using SADI restraints on equivalent bonds and FLAT restraints on symmetry-equivalent carbon atoms to contain the molecule to *D<sub>5h</sub>* symmetry. The fullerene in structure **6** was refined with same distance restraints, SADI, corresponding to *D<sub>5h</sub>* symmetry.

All atoms were allowed to assume anisotropic motion, but free refinement was unstable, and the U<sub>ij</sub> components of the fullerenes were restrained using SIMU. Hydrogen atoms were introduced at calculated positions and allowed to ride on the carrier atom with U<sub>iso</sub> 20% greater than U<sub>eq</sub>.

For **7**, a black fragment (0.56 × 0.48 × 0.30 mm) of a thick platelike crystal was used for the single-crystal X-ray diffraction study. The crystal was coated with epoxy resin to prevent the loss of the solvent of crystallization. The X-ray intensity data were collected at 198 K on a Bruker SMART 1000 CCD-based X-ray diffractometer system<sup>31</sup> with a Mo-target X-ray tube (λ = 0.71073) operated at 2000 W power. The CCD detector was placed at a distance of 3.455 cm from the crystal.

A total of 1818 frames were collected for a sphere of reflections with a scan width of 0.3° in ω and with φ angles of 0, 120, and 240° for every 606 frames. The exposure time was 30 s/frame. The frames were integrated with the Bruker SAINTPLUS software package<sup>32</sup> using a narrow-frame integration algorithm. Using a triclinic crystal system, the integrated frames yielded a total of 35 649 reflections at a maximum 2θ angle of 45° (0.928 Å resolution), of which 14 544 were independent reflections (*R*<sub>int</sub> = 0.0339, *R*<sub>sig</sub> = 0.0401, redundancy 2.11, 100% complete) and 10 587 (72.8%) reflections were greater than 2σ(*I*). The final cell constants were: *a* = 17.1863(9) Å, *b* = 17.9860(10) Å, *c* = 21.3379(12) Å, α = 114.5610(10)°, β = 99.7720(10)°, γ = 103.5240(10)°, *V* = 5560.6(5) Å<sup>3</sup>, calculated density *D<sub>c</sub>* = 1.549 g/cm<sup>3</sup>. Absorption corrections were applied to the raw reflections using the SADABS program in the Bruker SAINTPLUS software package.

The Bruker SHELXTL (version 5.1) software package<sup>33</sup> was used for phase determination and structure refinement. The distribution of intensities (*E*<sup>2</sup> - 1 = 0.921) indicated two possible space groups; *P*1 and *P*-1. The combined figure of merits indicated *P*-1 to be the most likely space group, which was later determined to be correct. The Patterson method was used to identify the two nickel atoms. With subsequent isotropic refinement, all the nonhydrogen atoms were identified in the asymmetric unit of the unit cell. The two nickel atoms were located at two different inversion centers. The asymmetric unit of the unit cell contains two halves of Ni porphyrin, two C<sub>70</sub> fullerenes, and two toluene molecules as solvents of crystallization. One of the two C<sub>70</sub> molecules is disordered, with the disorder occupancy factors being 76% and 24%. The polar 5-fold axes of these two disordered C<sub>70</sub> molecules are tilted by approximately 41° relative to each other. One of the two toluenes is also disordered, with the disorder occupancy factors being 85 and 15%.

Atomic coordinated, isotropic, and anisotropic temperature factors of all nonhydrogen atoms were refined by means of full-matrix least squares procedures. The 70 C atoms of the 24% occupied fullerene and the C atom of the methyl group of the 15% occupied toluene were refined isotropically because anisotropic refinement of these atoms was unstable. The C atoms of the 76% occupied fullerene were refined anisotropically using the DELU-restraining parameter. The C atoms of the nondisordered fullerene and the rest of the toluene C atoms were refined anisotropically using the SIMU-restraining parameter. The bond lengths of all the different layers of C atoms of each fullerene were refined using different SADI-restraining parameters. The SAME-restraining parameter was used to fix the disordered toluene molecules relative to the nondisordered toluene molecule. The H-atoms were included in the refinement in calculated positions riding on the atoms to which they are attached. The refinement converged at *R* = 0.0705, *R<sub>w</sub>* = 0.1765, with *I* > 2σ(*I*). The largest peak in the final difference map was 0.772 e/Å<sup>3</sup>.

**H<sub>2</sub>TTPP·C<sub>60</sub>·3 toluene, 1:** C<sub>125</sub>H<sub>54</sub>N<sub>4</sub>, fw = 1611.83, Triclinic, *P*-1, *a* = 14.2783(3) Å, *b* = 16.7220(3) Å, *c* = 17.0596(3) Å, α = 69.1150(10)°, β = 85.3380(10)°, γ = 78.1640(10)°, *V* = 3724.51(12) Å<sup>3</sup>, *Z* = 2, *D<sub>c</sub>* = 1.437 g/cm<sup>3</sup>, 2θ<sub>max</sub> = 56.6°, 12 970 measured reflections of which 8445 with *I* > 2σ(*I*) were used for refinement to give *R* = 0.0867, *R<sub>w</sub>* = 0.2489, and GOF = 1.069.

**H<sub>2</sub>T<sub>3,5</sub>-dibutylPP·C<sub>60</sub>, 2:** C<sub>136</sub>H<sub>94</sub>N<sub>4</sub>, fw = 1784.27, Orthorhombic, *Pbcn*, *a* = 14.6500(4) Å, *b* = 28.9181(9) Å, *c* = 22.8385(7) Å, *V* = 9675.5(5) Å<sup>3</sup>, *Z* = 4, *D<sub>c</sub>* = 1.225 g/cm<sup>3</sup>, 2θ<sub>max</sub> = 53.0°, 8535 measured reflections of which 5822 with *I* > 2σ(*I*) were used for refinement to give *R* = 0.092, *R<sub>w</sub>* = 0.233, and GOF = 1.032.

**H<sub>2</sub>T<sub>3,5</sub>-dimethylPP·1.5C<sub>60</sub>·2 toluene, 3:** C<sub>156</sub>H<sub>62</sub>N<sub>4</sub>, fw = 1992.24, Monoclinic, *C2/m*, *a* = 26.5840(2) Å, *b* = 23.8373(2) Å, *c* = 15.3327(2) Å, β = 106.5520(10)°, *V* = 9313.56(16) Å<sup>3</sup>, *Z* = 4, *D<sub>c</sub>* = 1.421 g/cm<sup>3</sup>, 2θ<sub>max</sub> = 52.9°, 8393 measured reflections of which 5656 with *I* > 2σ(*I*) were used for refinement to give *R* = 0.0923, *R<sub>w</sub>* = 0.2889, and GOF = 1.07.

**H<sub>2</sub>T<sub>pin</sub>PP·C<sub>60</sub>, 4:** C<sub>124</sub>H<sub>66</sub>N<sub>8</sub>O<sub>4</sub>, fw = 1731.85, Monoclinic, *C2/c*, *a* = 20.7187(4) Å, *b* = 17.9498(3) Å, *c* = 23.0134(3) Å, β = 104.9190(10)°, *V* = 8270.1(2) Å<sup>3</sup>, *Z* = 4, *D<sub>c</sub>* = 1.391 g/cm<sup>3</sup>, 2θ<sub>max</sub> = 52.88°, 7219 measured reflections of which 3897 with *I* > 2σ(*I*) were used for refinement to give *R* = 0.0876, *R<sub>w</sub>* = 0.1966, and GOF = 1.019.

**H<sub>2</sub>T<sub>3,5</sub>-dimethylPP·C<sub>70</sub>·4 toluene, 5:** C<sub>150</sub>H<sub>78</sub>N<sub>4</sub>, fw = 1936.15, Triclinic, *P*-1, *a* = 12.7502(3) Å, *b* = 14.5740(4) Å, *c* = 15.4166(4) Å, α = 117.9350(10)°, β = 100.4670(10)°, γ = 97.1790(10)°, *V* = 2414.96(11) Å<sup>3</sup>, *Z* = 1, *D<sub>c</sub>* = 1.331 g/cm<sup>3</sup>, 2θ<sub>max</sub> = 52.88°, 8283 measured reflections of which 5683 with *I* > 2σ(*I*) were used for refinement to give *R* = 0.1430, *R<sub>w</sub>* = 0.364, and GOF = 1.058.

**ZnTTPP·C<sub>70</sub>, 6:** C<sub>114</sub>H<sub>28</sub>N<sub>4</sub>Zn, fw = 1518.89, Triclinic, *P*-1, *a* = 14.48050(10) Å, *b* = 16.5025(2) Å, *c* = 17.7287(3) Å, α = 72.6230(10)°, β = 86.58°, γ = 80.5740(10)°, *V* = 3988.32(9) Å<sup>3</sup>, *Z* = 2, *D<sub>c</sub>* = 1.260 g/cm<sup>3</sup>, 2θ<sub>max</sub> = 50.0°, 13 752 measured reflections of which 10 338 with *I* > 2σ(*I*) were used for refinement to give *R* = 0.1016, *R<sub>w</sub>* = 0.2901, and GOF = 1.152.

**NiT<sub>4</sub>-methylPP·2C<sub>70</sub>·2 toluene, 7:** C<sub>202</sub>H<sub>52</sub>N<sub>4</sub>Ni, fw = 2593.36, Triclinic, *P*-1, *a* = 17.1863(9) Å, *b* = 17.9860(10) Å, *c* = 21.3379(12) Å, α = 114.5610(10)°, β = 99.7720(10)°, γ = 103.5240(10)°, *V* = 5560.6(5) Å<sup>3</sup>, *Z* = 2, *D<sub>c</sub>* = 1.549 g/cm<sup>3</sup>, 2θ<sub>max</sub> = 45.0°, 35 649 measured reflections of which 10 587 with *I* > 2σ(*I*) were used for refinement to give *R*<sub>1</sub> = 0.0705, *R<sub>w</sub>* = 0.1765, and GOF = 1.029.

Further crystallographic details, atomic coordinates for all nonhydrogen atoms, anisotropic thermal parameters, and fixed hydrogen atom coordinates are given in tables in the Supporting Information.

**Density Functional Calculations.** Density functional calculations were performed using Amsterdam Density Functional program.<sup>19</sup> Double basis sets were used for C(2s, 2p), N(2s, 2p), and H(1s) augmented by a single 3d polarization function. The inner electron configurations were assigned to the core and were treated using the frozen core approximation. Calculations were carried out with the local exchange-correlation potential due to Vosko, Wilk, and Nusair<sup>34</sup> using nonlocal corrections for the exchange due to Becke<sup>35</sup> with nonlocal corrections for the correlation due to Lee, Yang, and Parr.<sup>36</sup> Binding energies were calculated from the energy of interaction of a fullerene/porphyrin cluster using the density functional model. The geometries of these clusters were taken from the X-ray crystal structures of **1** and **5**.

**Molecular Modeling Using Force Fields.** Clusters of fullerenes with porphyrins of various sizes were constructed from the experimentally observed arrangements in the X-ray structures or by construction in the modeling program Cerius2.<sup>16</sup> The minimum energy structures with respect to the universal force field<sup>17</sup> were then calculated. Similar structures were obtained by both methods.

**Acknowledgment.** We thank Dr. A. K. Burrell (Massey University) for samples of 3,5-dimethylphenyl- and 3,5-di-*tert*-

(31) SMART Software Reference Manual, version 5.054; Bruker Analytical X-ray Systems, Inc.: Madison, WI, 1997–1998.

(32) SAINTPLUS Software Reference Manual, version 5.02; Bruker Analytical X-ray Systems, Inc.: Madison, WI, 1997–1998.

(33) SHELXTL Software Reference Manual, version 5.1; Bruker Analytical X-ray Systems, Inc.: Madison, WI, 1997–1998.

(34) Vosko, S. H.; Wilk, L.; Nusair, M. *Can. J. Phys.* **1980**, *58*, 1200–1211.

(35) Becke, A. D. *Phys. Rev. A: Gen. Phys.* **1988**, *38*, 3098.

(36) Lee, C.; Yang, W.; Parr, R. G. *Phys. Rev. B: Condens. Matter* **1988**, *37*, 785.

butylphenyl-porphyrins and Professor A. L. Balch for a preprint of ref 21. This work was supported by the Marsden Fund of New Zealand (UOA613) administered by the Royal Society of New Zealand, the University of Auckland Research Committee, and the National Institutes of General Medical Sciences. C. A. R. thanks the John Simon Guggenheim Foundation for Fellowship support while this paper was written. F. S. T. thanks Dr. M. M. Olmstead for helpful discussions.

**Supporting Information Available:** Full crystallographic details, atomic coordinates, anisotropic displacement coefficients, H atom coordinates, and atom numbering schemes. This information is available free of charge via the Internet at <http://pubs.acs.org>.

JA992165H